

# Multifunctional ceramics $\text{Ba}_{1-x}\text{Sr}_x(\text{Ti}_{1-x}\text{Li}_x)\text{O}_{3-3x}\text{F}_{3x}$

Meriem Meyar, Laldja Taïbi-Benziada\*

Faculty of Chemistry, USTHB, P.O. Box 32 El-Alia, Bab-Ezzouar, 16311 Algiers, Algeria

Available online 13 June 2006

## Abstract

Mixtures of  $(1-x)\text{BaTiO}_3 + x\text{SrF}_2 + x\text{LiF}$  are prepared and dry-ground. The powders thus obtained are shaped to discs and sintered in free-air at  $950^\circ\text{C}$  for 2 h. The shrinkage coefficient varies between 14.5% and 16.8%. The XRD patterns show the formation of a new solid solution with general formula  $\text{Ba}_{1-x}\text{Sr}_x(\text{Ti}_{1-x}\text{Li}_x)\text{O}_{3-3x}\text{F}_{3x}$  which occurs in the composition range  $0 \leq x \leq 0.25$ . The ceramic grain size is observed by Scanning Electron Microscopy (SEM) on fractured samples. The phase transitions in these perovskite-type oxifluorides are investigated by Differential Scanning Calorimetry (DSC) and dielectric measurements. The sintering temperature ( $t_{\text{sin}} \approx 1400^\circ\text{C}$ ) and the ferroelectric Curie temperature ( $T_C \approx 120^\circ\text{C}$ ) of  $\text{BaTiO}_3$  are strongly lowered by the triple substitution Ba–Sr, Ti–Li and O–F. The value of  $T_C$  for  $\text{Ba}_{0.95}\text{Sr}_{0.05}(\text{Ti}_{0.95}\text{Li}_{0.05})\text{O}_{2.85}\text{F}_{0.15}$  is around  $-65^\circ\text{C}$ . These new phases are suitable for the fabrication of capacitors in various microelectronic devices.

© 2006 Elsevier Ltd. All rights reserved.

**Keywords:**  $\text{Ba}_{1-x}\text{Sr}_x(\text{Ti}_{1-x}\text{Li}_x)\text{O}_{3-3x}\text{F}_{3x}$  ceramics

## 1. Introduction

In recent years, ferroelectric compounds attracted more and more researchers and industrials because they became the key of success in the huge market of electronic devices. Among this family, barium titanate ( $\text{BaTiO}_3$ ) is a ferroelectric perovskite below  $120^\circ\text{C}$  with a sequence of phase transitions<sup>1</sup> and a high dielectric permittivity (about 1000–2000) at room temperature. These characteristics make this material of an interest in several technological applications such as: Multilayer Ceramic Capacitors, MLCCs,<sup>2,3</sup> sensors of gas pollution like  $\text{CO}$ ,<sup>4</sup> thermistors<sup>5</sup> and Ferroelectric Random Access Memories FRAMs.<sup>6</sup>

$\text{BaTiO}_3$  is conventionally synthesized and sintered at high temperature ( $T \geq 1400^\circ\text{C}$ ) by solid state reaction between  $\text{BaCO}_3$  and  $\text{TiO}_2$ . In such conditions, the control of the grain size is difficult. On the other hand, in the manufacture of multilayer capacitors, the high temperature formation leads to the use of expensive metals as electrodes (Pd or Pt). New techniques of preparation at temperatures lower than  $1000^\circ\text{C}$  allowed the replacement of palladium and platinum electrodes by cheap metals or metal alloys in the production of capacitors. Beyond these techniques one can cite as examples wet chemical processes like sol–gel, hydrothermal or ACS methods to get very pure  $\text{BaTiO}_3$  with very fine particles.<sup>7–10</sup>

Since approximately two decades, the solid state reaction is developed too, either for the improvement of dielectric properties of barium titanate thanks to fluorides as sintering additives<sup>11,12</sup> or to get  $\text{BaTiO}_3$  powder with high crystallinity and fine particles.<sup>13</sup>

The purpose of this work is first of all to synthesize new phases  $(\text{Ba}, \text{Sr})(\text{Ti}, \text{Li})(\text{O}, \text{F})_3$ , then to determine the effect of  $(\text{SrF}_2 + \text{LiF})$  addition on the sintering and the physical properties of  $\text{BaTiO}_3$ .

## 2. Starting products and ceramic preparation

Chemically pure barium carbonate (99.9%), titanium dioxide (99.9%) and suprapure fluorides  $\text{SrF}_2$  and  $\text{LiF}$  are all purchased from MERCK.  $\text{BaCO}_3$  and  $\text{TiO}_2$  are heat-treated at  $300^\circ\text{C}$  during three days to eliminate any trace of humidity.  $\text{SrF}_2$  and  $\text{LiF}$  are treated at  $150^\circ\text{C}$  under vacuum for several hours to prevent any hydrolysis of fluorides during sintering.

The powder of  $\text{BaTiO}_3$  is prepared by calcination of a stoichiometric mixture of  $\text{BaCO}_3$  and  $\text{TiO}_2$  at  $1100^\circ\text{C}$ . Then, various amounts of  $(\text{SrF}_2 + \text{LiF})$  are added to  $\text{BaTiO}_3$  to obtain molar mixtures of  $(1-x)\text{BaTiO}_3 + x\text{SrF}_2 + x\text{LiF}$ . These mixtures are homogenized and dry-ground with an agate mortar during (1/2) hour. After that, they are shaped to discs of 13 mm diameter and about 1 mm thickness by pressing under approximately  $10^8$  Pa without a binder. These pellets are sintered in free-air at  $950^\circ\text{C}$

\* Corresponding author. Fax: +213 21 24 73 11.  
E-mail address: [ikra@wissal.dz](mailto:ikra@wissal.dz) (L. Taïbi-Benziada).

Table 1  
Shrinkage and XRD data of  $\text{Ba}_{1-x}\text{Sr}_x(\text{Ti}_{1-x}\text{Li}_x)\text{O}_{3-3x}\text{F}_{3x}$  phases

Composition	$\Delta\Phi/\Phi$	$a$ (Å)	$V$ (Å <sup>3</sup> )
$\text{BaTiO}_3$	5.38	4.0638(5)	67.1115
$\text{Ba}_{0.95}\text{Sr}_{0.05}(\text{Ti}_{0.95}\text{Li}_{0.05})\text{O}_{2.85}\text{F}_{0.15}$	14.5	4.0049(6)	64.2359
$\text{Ba}_{0.90}\text{Sr}_{0.10}(\text{Ti}_{0.90}\text{Li}_{0.10})\text{O}_{2.70}\text{F}_{0.30}$	15.4	3.9991(6)	63.9587
$\text{Ba}_{0.85}\text{Sr}_{0.15}(\text{Ti}_{0.85}\text{Li}_{0.15})\text{O}_{2.55}\text{F}_{0.45}$	15.8	3.9912(8)	63.5813
$\text{Ba}_{0.80}\text{Sr}_{0.20}(\text{Ti}_{0.80}\text{Li}_{0.20})\text{O}_{2.40}\text{F}_{0.60}$	16.8	3.9864(4)	63.3508

for 2 h. The shrinkage of the resultant ceramics is in the range 14.5–16.8%.

### 3. X-ray diffraction study

An X-ray diffraction study is performed at room temperature on crushed ceramics to fine powder, with a PHILIPS PW1710 diffractometer using  $\text{Cu K}\alpha_1$  radiation ( $\lambda = 1.54056 \text{ Å}$ ) as X-ray source. The angle range ( $2\theta$ ) is investigated between 5 and  $80^\circ$ .

The XRD patterns show no secondary phases in the samples for  $x \leq 0.25$ . All the ceramics are single-phased with a perovskite structure in a wide composition range ( $0 \leq x \leq 0.25$ ).

The main peaks of (Ba, Sr)(Ti, Li)(O, F)<sub>3</sub> are close to those of cubic unsubstituted  $\text{BaTiO}_3$  reported in the ASTM cards (American Society for Testing Materials). The unit cell parameter  $a$  of  $\text{Ba}_{1-x}\text{Sr}_x(\text{Ti}_{1-x}\text{Li}_x)\text{O}_{3-3x}\text{F}_{3x}$  phases is calculated from the (100) and (110) peak spacings. After that, they are computer affined using a program basing on the least squares method. The results are reported in Table 1.

The variations of the lattice parameter  $a$  and volume  $V$  with  $x$  are not significant. The increase size from  $\text{Ti}^{4+}$  to  $\text{Li}^+$  in octahedron sites ( $r(\text{Ti}^{4+}) = 0.60 \text{ Å}$ ,  $r(\text{Li}^+) = 0.74 \text{ Å}$ ) is compensated by the decrease size from  $\text{O}^{2-}$  to  $\text{F}^-$  ( $r(\text{O}^{2-}) = 1.40 \text{ Å}$ ,  $r(\text{F}^-) = 1.33 \text{ Å}$ ). The slight decrease in  $a$  and  $V$  is attributed to the diminution of cation size in dodecahedron sites ( $r(\text{Ba}^{2+}) = 1.60 \text{ Å}$ ,  $r(\text{Sr}^{2+}) = 1.44 \text{ Å}$ ).

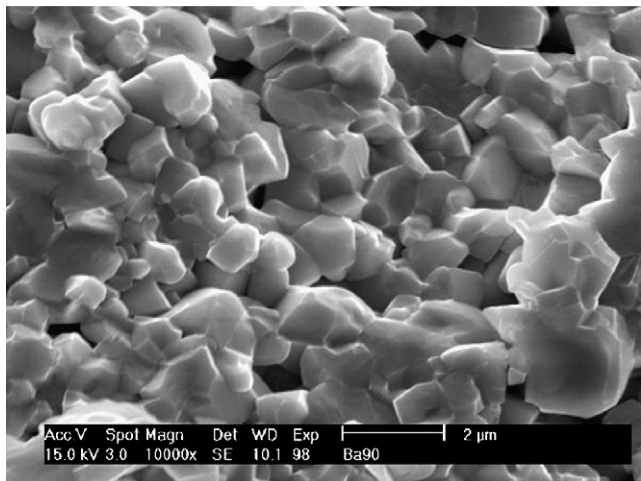


Fig. 1. Microstructure of  $\text{Ba}_{0.90}\text{Sr}_{0.10}(\text{Ti}_{0.90}\text{Li}_{0.10})\text{O}_{2.70}\text{F}_{0.30}$  ceramic.

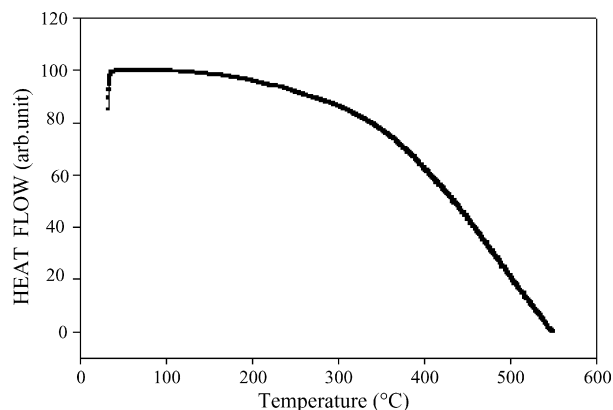


Fig. 2. DSC curve of  $\text{Ba}_{0.90}\text{Sr}_{0.10}(\text{Ti}_{0.90}\text{Li}_{0.10})\text{O}_{2.70}\text{F}_{0.30}$  sample.

### 4. Shrinkage and microstructures

After sintering, the ceramic diameter ( $\Phi$ ) is measured to obtain the shrinking coefficient ( $\Delta\Phi/\Phi$ ) for the estimation of the sample compactness.

Microstructure observations are carried out on fractured ceramics using a PHILIPS ESEM FEG XL 30 microscope. All fluorinated ceramics  $\text{Ba}_{1-x}\text{Sr}_x(\text{Ti}_{1-x}\text{Li}_x)\text{O}_{3-3x}\text{F}_{3x}$  show good shrinkages by sintering at  $950^\circ\text{C}$  for 2 h whereas the value

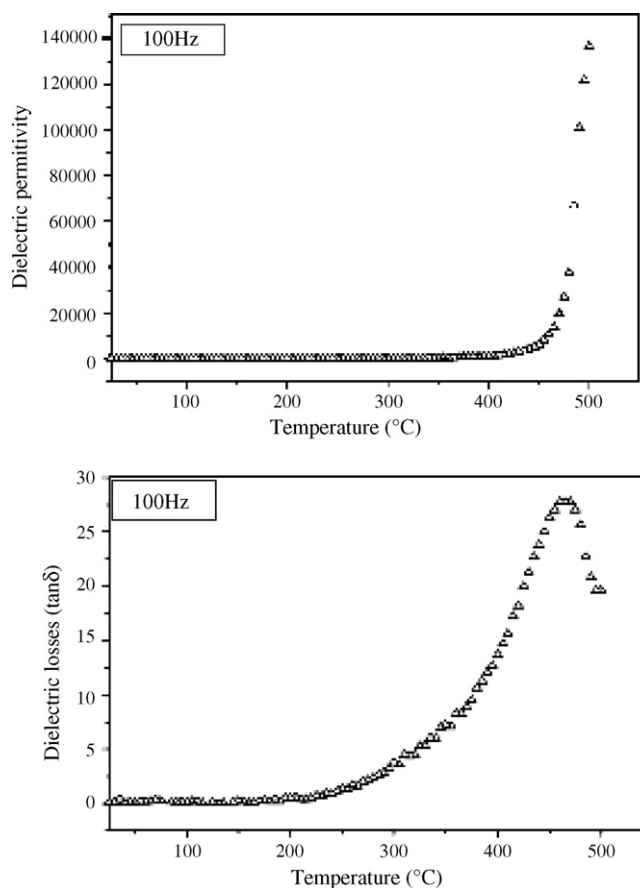


Fig. 3. Temperature dependence of  $\epsilon'_r$  and  $\tan \delta$  of  $\text{Ba}_{0.90}\text{Sr}_{0.10}(\text{Ti}_{0.90}\text{Li}_{0.10})\text{O}_{2.70}\text{F}_{0.30}$  ceramic (100 Hz).

of  $\Delta\Phi/\Phi$  for pure BaTiO<sub>3</sub> sintered in the same conditions is low (Table 1) and the corresponding ceramic is friable. As the fluorine concentration increases, the material becomes more refractory. During the sintering process, the additive (SrF<sub>2</sub> + LiF) act simultaneously as substituant in the host lattice where Sr, Li and F elements replace, respectively Ba, Ti and O crystallographic sites and as agent of sintering at low temperature. No interior or surface second phases are found on the ceramic micrographs. These results agree quite well with those of the XRD study. The porosity is intergranular for all the compositions. The size of grains is not regular. For example, Fig. 1 shows the microstructure of Ba<sub>0.90</sub>Sr<sub>0.10</sub>(Ti<sub>0.90</sub>Li<sub>0.10</sub>)O<sub>2.70</sub>F<sub>0.30</sub> ceramic. As it may be seen, the structure is dense with intergranular pores. The grain size is in the range 0.5  $\mu\text{m}$ –2  $\mu\text{m}$ .

## 5. DSC analyses

Differential Scanning Calorimetry (DSC) analyses are performed under nitrogen gas (N<sub>2</sub>) from room temperature up to 600 °C with a PERKEN-ELMER apparatus and a heating rate of 10 °C/min. No phenomenon is observed in the temperature range investigated whatever the composition is. A typical DSC curve is illustrated in Fig. 2.

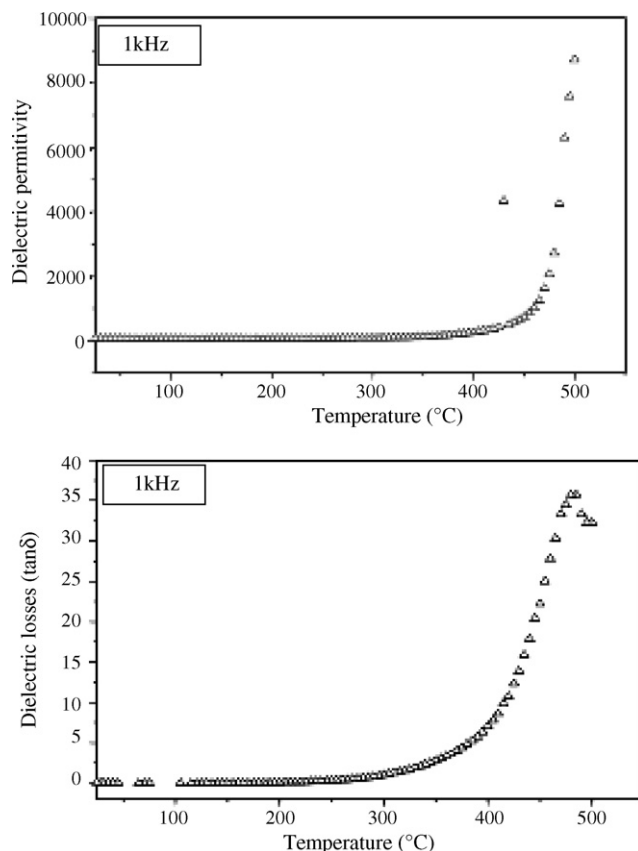


Fig. 4. Temperature dependence of  $\epsilon'_r$  and  $\tan \delta$  of Ba<sub>0.90</sub>Sr<sub>0.10</sub>(Ti<sub>0.90</sub>Li<sub>0.10</sub>)O<sub>2.70</sub>F<sub>0.30</sub> ceramic (1 kHz).

## 6. Dielectric measurements

In a first study, capacitors are prepared from pre-sintered pellets by depositing thin silver layers as electrodes onto the opposite circular faces. The dielectric permittivity  $\epsilon'_r$  and losses  $\tan \delta$  are measured from 500 °C down to room temperature at 100 Hz or 1 kHz. The measurements are carried out under nitrogen gas (N<sub>2</sub>) with a cooling rate of 5 °C/min using a LCR data automatic bridge.

The curves  $\epsilon'_r - T$  and  $\tan \delta - T$  exhibit the same profile whatever the value of  $x$  or the frequency is. The curves are very flat over a large range of temperature (25–300 °C) with a strong increase beyond  $\sim 300$ –400 °C. As example, Figs. 3 and 4 give the temperature dependence of  $\epsilon'_r$  and  $\tan \delta$  for Ba<sub>0.90</sub>Sr<sub>0.10</sub>(Ti<sub>0.90</sub>Li<sub>0.10</sub>)O<sub>2.70</sub>F<sub>0.30</sub> ceramic, respectively at 100 and 1 kHz. No phase transition is observed in the temperature range investigated. The increasing in  $\epsilon'_r$  and  $\tan \delta$  at high temperatures (beyond  $\sim 300$  °C) is attributed to the electrical conductivity of lithium ion Li<sup>+</sup> which is about  $10.8 \times 10^6 \Omega^{-1} \text{m}^{-1}$ . The values of the dielectric permittivity and losses at room temperature are compatible with the specifications of type I materials for capacitors.

All the oxyfluorides Ba<sub>1-x</sub>Sr<sub>x</sub>(Ti<sub>1-x</sub>Li<sub>x</sub>)O<sub>3-3x</sub>F<sub>3x</sub> are paraelectric at room temperature. The ferroelectric peak of pure

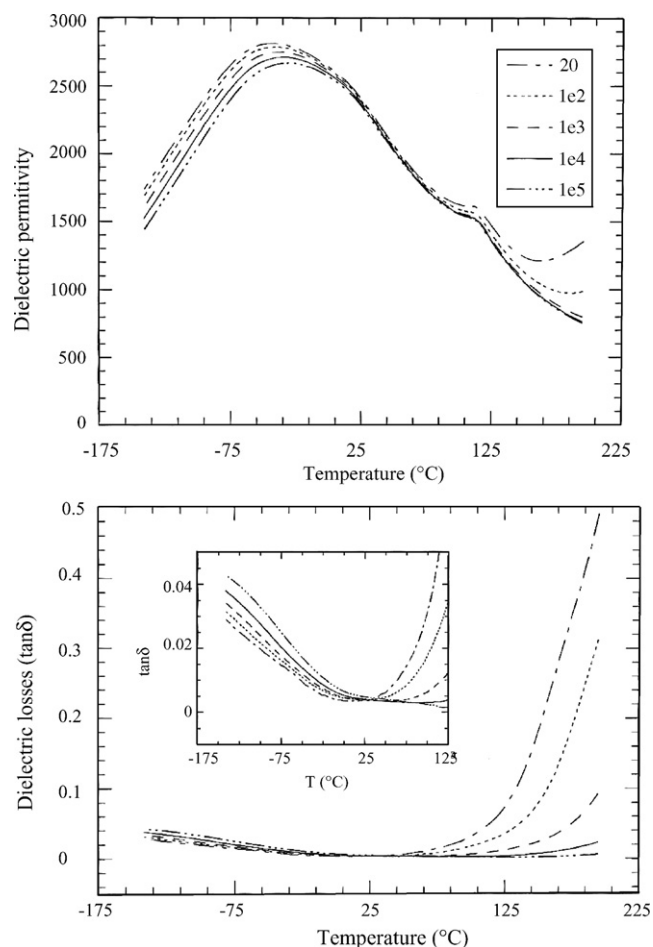


Fig. 5. Temperature dependence of  $\epsilon'_r$  and  $\tan \delta$  of Ba<sub>0.95</sub>Sr<sub>0.05</sub>(Ti<sub>0.95</sub>Li<sub>0.05</sub>)O<sub>2.85</sub>F<sub>0.15</sub> ceramic at various frequencies.

BaTiO<sub>3</sub> ( $T_C \approx 120^\circ\text{C}$ ) is certainly shifted at very low temperature by the substitution O–F as it was shown in our previous works.<sup>3,11,12,14</sup>

To confirm this hypothesis, a second dielectric study is performed on the ceramic with less fluorine concentration ( $x = 0.05$ ). Gold electrodes are sputter deposited on the polished circular surfaces of the pellet. The measurements are carried out in cooling regime from  $225^\circ\text{C}$  down to  $-175^\circ\text{C}$  with a rate of  $1^\circ\text{C}/\text{min}$ , using an HP 4284A LCR meter which operates at five frequencies: 20,  $10^2$ ,  $10^3$ ,  $10^4$  and  $10^5$  Hz. As it may be seen in Fig. 5, a very broad maximum of  $\varepsilon'_r$  appears around  $-65^\circ\text{C}$ . For larger amounts of fluorine, the value of  $T_C$  is of course much lower.

## 7. Conclusion

The investigations of the chemical system BaTiO<sub>3</sub>–SrF<sub>2</sub>–LiF allowed us to synthesize a novel fluorinated solid solution with general formula Ba<sub>1–x</sub>Sr<sub>x</sub>(Ti<sub>1–x</sub>Li<sub>x</sub>)O<sub>3–3x</sub>F<sub>3x</sub>. This occurs in the composition range  $0 \leq x \leq 0.25$ . During the sintering process, the diffraction pattern of tetragonal barium titanate is transformed in a cubic one by the triple substitution Ba–Sr, Ti–Li and O–F. The SrF<sub>2</sub> + LiF additive lowers simultaneously the sintering temperature of pure BaTiO<sub>3</sub> from about  $1400$  to  $950^\circ\text{C}$  and the ferroelectric Curie temperature from  $\sim 120^\circ\text{C}$  to values less than room temperature ( $T_C < 25^\circ\text{C}$ ). These new oxifluorides are promising materials for fabrication of capacitors in various microelectronic devices.

## Acknowledgements

The authors acknowledge Dr. Belkadi, M., Dr. Mezroua A. and Dr. Souami N. for their kind help in the physical characterizations.

## References

- Goddard, W. A., Zhang, Q., Uludogan, M., Strachan, A. and Cagin, T., The ReaxFF polarizable reactive force fields for molecular dynamics simulation of ferroelectrics. *Fund. Phys. Ferroelectrics*, 2002.
- Yoon, D. H. and Lee, B. I., Processing of barium titanate tapes with different binders for MLCC applications. Part II: Comparison of the properties. *J. Eur. Ceram. Soc.*, 2004, **24**, 753–761.
- Taïbi-Benziada, L., Ferroelectric ceramics related to BaTiO<sub>3</sub> for Z5U multilayer capacitors. *Mater. Sci. Forum*, 2005, **492–493**, 109–114.
- Zhou, Z. G., Tang, Z. L. and Zhang, Z. T., Impedance analysis study on the sensing process of BaTiO<sub>3</sub> based PTC ceramics in CO gas. *Key Eng. Mater.*, 2005, **280–283**, 369–372.
- Li, Z. C. and Bergman, B., Thermal cycle characteristics of PTCR ceramic thermistors. *Sensor Actuat. A*, 2005, **118**, 92–97.
- Scott, J. F., New developments on FRAMs: [3D] structures and all-perovskite FETs. *Mater. Sci. Eng. B*, 2005, **120**(1–3), 6–12.
- Pfaff, G., Sol-gel synthesis of barium titanate powders of various compositions. *J. Mater. Chem.*, 1992, **2**(6), 591–594.
- McHale, J. M., McIntyre, P. C., Sickafus, K. E. and Coppa, N. V., Nanocrystalline BaTiO<sub>3</sub> from freeze-dried nitrate solutions. *J. Mater. Res.*, 1996, **11**(5), 1199–1209.
- Hu, M. Z. C., Kurian, V., Payzant, E. A., Rawn, C. J. and Hunt, R. D., Wet-chemical synthesis of monodispersed barium titanate particules-hydrothermal conversion of TiO<sub>2</sub> microspheres to nanocrystalline BaTiO<sub>3</sub>. *Powder Technol.*, 2000, **110**, 2–14.
- Lee, B. I., Wang, M. X. and Yoon, D. H., Some current processing issues in barium titanate powders. *Key Eng. Mater.*, 2004, **264–268**, 9–14.
- Benziada-Taïbi, L., Ravez, J. and Hagenmuller, P., Influence de l'ajout de BaLiF<sub>3</sub> sur les propriétés cristallographiques et diélectriques de BaTiO<sub>3</sub>. *J. Fluo. Chem.*, 1984, **26**, 395–404.
- Benziada, L. and Ravez, J., Ferroelectric BaTiO<sub>3</sub> ceramics sintered at low temperature with the aid of a mixture of CaF<sub>2</sub> and LiF. *J. Fluo. Chem.*, 1995, **73**, 69–71.
- Ando, C., Chazono, H. and Kishi, H., Effect of particle size and mixing homogeneity of starting powder on solid state synthesis of BaTiO<sub>3</sub>. *Key Eng. Mater.*, 2004, **269**, 161–164.
- Benziada, L. and Claverie, J., Influence of the eutectic composition 1CaF<sub>2</sub>–4LiF on the sintering and the dielectric properties of BaTiO<sub>3</sub>. *Ferroelectrics*, 1996, **189**, 129–138.